PHYSICAL REVIEW A **72**, 020301(R) (2005)

Geometric quantum gates that are robust against stochastic control errors

Shi-Liang Zhu[1,2,3] and Paolo Zanardi[1]

[1]*Institute for Scientific Interchange Foundation, Viale Settimio Severo 65, I-10133 Torino, Italy*

[2]*School of Physics and Telecommunication Engineering, South China Normal University, Guangzhou, China*

[3]*FOCUS Center and MCTP, Department of Physics, University of Michigan, Ann Arbor, Michigan 48109, USA*

(Received 26 July 2004; published 15 August 2005)

The realistic application of geometric quantum computation is crucially dependent on an unproved robustness conjecture, claiming that geometric quantum gates are more resilient against random noise than dynamic gates. We propose a suitable model that allows a direct and fair comparison between geometrical and dynamical operations. In the presence of stochastic control errors we find that the maximum of gate fidelity corresponds to quantum gates with a vanishing dynamical phase. This is a clear evidence for the robustness of nonadiabatic geometric quantum computation. The predictions here presented can be experimentally tested in almost all of the already existing quantum computer candidates.

DOI: 10.1103/PhysRevA.72.020301 PACS number(s): 03.67.Lx, 03.65.Vf, 03.67.Pp

An essential prerequisite for quantum computation (QC) is the ability to maintain quantum coherence and quantum entanglement in an information-processing system [1]. Unfortunately, since both these properties are very fragile against control errors as well as against unwanted couplings with environment, this goal is extremely hard to achieve. To this end several strategies have been developed, most notably quantum error correction [2], decoherence-free subspace [3], and bang-bang techniques (dynamical suppression of decoherence) [4].

Quantum computation implemented by geometric phases [5] is believed to be another approach that can be used to overcome certain kinds of errors [6–10]. However, the statement that quantum gates (QGs) achieved by this way may have built-in fault-tolerant features (due to the fact that geometric phases depend only on some global geometric properties) has still the status of a debated conjecture. Indeed this alleged resilience against errors of geometrical gates has been doubted by some numerical calculations including certain decohering mechanisms [11,12]. On the other hand, analytical results show that the adiabatic Berry's phase itself may be robust against dephasing [13] and stochastic fluctuations of control parameters [14]. These latter provide a sort of indirect evidence for the robustness of adiabatic geometric QC, but a more direct and convincing evidence is still missing. Since any realistic application of geometric QC is crucially dependent on this robustenss conjecture, to prove or to reject it unavoidably becomes one of the key tasks in the field of geometric QC.

In this paper we analyze a scheme for QC that is suitable to distinguish the difference between geometric QGs and dynamic gates and then provide a clear-cut evidence for the robustness of nonadiabatic geometric QC. The main points we are going to make are the following:

(i) The main difficulty in proving or rejecting the robustness conjecture is that one does not have a suitable model that allows a direct and fair comparison between geometrical and dynamical operations. The difficulty is overcome by the model analyzed here. The model is, in a sense, a hybrid between the purely geometric QG and the standard dynamic one; by tuning the parameters, the QGs can be continuously changed from one kind to theother. Thus, studying the changes of the fidelity in the presence of noise allows one to distinguish which kind of gates perform better, in a direct fashion. From this perspective one may say that the model proposed is an ideal one to the aim of addressing the issue the difference of noise resilience between dynamic and geometric gates, regardless the actual outcome of the comparison.

(ii) In the presence of stochastic control errors, we find that the maximum of fidelity corresponds to those cases in which the dynamical phase accumulated over the gate operation is zero. This provides a clear evidence for the robustness of geometric QC.

(iii) This robustness feature may be significant to experiments on quantum information processing. Indeed it is generally believed that fluctuations of control parameters is one of the most dangerous sources of errors for qubits in solid-state systems [15], NMR [16], and trapped ions [17], etc.

Moreover, note that a general and standard Hamiltonian to describe almost all kinds of quantum computer prototypes is a Hamiltonian consisting of spin-half particles in the presence of (effective) magnetic fields, which is exactly what we addressed in this paper. Therefore, a further remarkable application is that the predictions presented here can be experimentally tested in almost all of the already existing quantum computer candidates, such as QC with NMR, trapped ions, quantum dots, and superconducting qubits, etc.

Quantum computation via a pair of orthogonal cyclic states. For universal QC, it is sufficient to enact two noncommuting single-qubit gates and one nontrivial two-qubit gate. Before studying the fidelity of a QG subject to noise, we recall a scheme to implement a universal set of QGs by using a pair of orthogonal cyclic states [8]. We consider a process in which a pair of orthogonal state $|\psi_\pm(t)\rangle$ evolve cyclically starting from $|\psi_\pm(0)\rangle$, i.e., $|\psi_\pm(\tau)\rangle = e^{\pm i\gamma}|\psi_\pm(0)\rangle$ with γ a real number. Any state at time τ is found to be $|\psi(\tau)\rangle = U_1|\psi(0)\rangle$, where [8]

$$U_1 = \begin{pmatrix} e^{i\gamma}\cos^2\frac{\chi}{2} + e^{-i\gamma}\sin^2\frac{\chi}{2} & i\sin\chi\sin\gamma \\ i\sin\chi\sin\gamma & e^{i\gamma}\sin^2\frac{\chi}{2} + e^{-i\gamma}\cos^2\frac{\chi}{2} \end{pmatrix}$$

is a single-qubit gate in the language of QC. Here χ is related to the initial state by $|\psi_+(0)\rangle = \cos\chi/2|0\rangle + \sin\chi/2|1\rangle$, and γ is a phase accumulated in the gate evolution. Moreover, a conditional two-qubit gate can also be implemented if there exist, conditional to the state of the control qubit, two different pairs of cyclic states of the target qubit. In terms of the computational basis $\{|00\rangle,|01\rangle,|10\rangle,|11\rangle\}$, where the first (second) bit represents the state of the control (target) qubit. The unitary operator describing the conditional two-qubit gate is given by $U_2 = \mathrm{diag}(U_1(\gamma^0,\chi^0),U_1(\gamma^1,\chi^1))$, under the condition that the control qubit is off resonance in the manipulation of the target qubit. Here γ^δ (χ^δ) represents the total phase (the cyclic initial state) of the target qubit when the control qubit is in the state $\delta(=0,1)$. Usually the total phase γ (γ^δ) consists of both geometric $(\gamma_g,\gamma_g^\delta)$ and dynamic components $(\gamma_d,\gamma_d^\delta)$ [5], and U_1 (U_2) is specified as a geometric gate if γ (γ^δ)) is a pure geometric phase. This scheme can be implemented in several realistic physical systems [8].

Control parameter fluctuation. A simple approach for implementing U_1 and U_2 is to use an effective rotating magnetic field to manipulate the state of qubits. In this case, the Hamiltonian for a single qubit reads

$$H = (\omega_0\sigma_x\cos\omega t + \omega_0\sigma_y\sin\omega t + \omega_1\sigma_z)/2, \qquad (1)$$

where $\omega_i = -g\mu B_i/\hbar$ $(i=0,1)$ with g (μ) being the gyromagnetic ratio (Bohr magneton), and B_i $(i=1,2)$ acts as an external controllable parameter, and its magnitude can be experimentally changed. We also use this Hamiltonian to manipulate the target qubit in the implementation of a two-qubit gate when the control qubit is off resonance. The Hamiltonian of the two-qubit system is given by the Hamiltonian (1) plus the coupling Hamiltonian acting on the two qubits. In the nonideal case the control fields contain randomly fluctuating components, here we assume that ω_i is flatly distributed in the interval $[(1-\delta_i)\omega_i,(1+\delta_i)\omega_i]$ with δ_i a constant, and then we numerically calculate the average fidelity of QGs U_1 and U_2. But we will assume that ω is not affected by random fluctuations; this seems reasonable since frequency may be well controlled in a realistic experiment.

The average fidelity of a QG we study is defined by

$$\bar{F} = \lim_{N\to\infty}\frac{1}{N}\sum_{j=1}^{N}\overline{F_j} = \lim_{N\to\infty}\frac{1}{N}\sum_{j=1}^{N}\overline{|\langle\psi_j^{in}|\hat{U}_{id}^\dagger|\psi_j^{out}\rangle|^2}, \qquad (2)$$

where $|\psi_j^{in}\rangle = [\cos(\theta_j/2)e^{-i\varphi_j/2},\sin(\theta_j/2)e^{i\varphi_j/2}]^T$ or $|\psi_j^{in}\rangle = [-\sin(\theta_j/2)e^{-i\varphi_j/2},\cos(\theta_j/2)e^{i\varphi_j/2}]^T$ (T denotes the matrix transposition) is an input state. $\theta_j\in[0,\pi]$ and $\varphi_j\in[0,2\pi]$ are randomly chosen in our numerical calculation. U_{id} is the ideal QG without any control parameter fluctuation and $|\psi_j^{out}\rangle$ is the output state after a noisy gate operation when the input state is $|\psi_j^{in}\rangle$. The action of the noisy gate is obtained by dividing the total operation time in I intervals, over each one of these ω_0 and ω_1 are randomly perturbed according the above described distributions. Since the noise is constant in each time interval, I^{-1} can be regarded as (proportional to) the noise correlation time.

In the numerical calculation, we randomly choose one input state $|\psi_j^{in}\rangle$, and then calculate the average fidelity of $\overline{F_j}$, up to satisfactory convergence, for M configurations of fluctuations of magnetic fields. After that, we randomly choose the next input state and repeat the above calculation until deriving the fidelity of this specific input state with satisfactory convergence. We repeat N times to calculate the average fidelity by randomly choosing $|\psi_j^{in}\rangle$. In our numerical calculations below, we get small statistical errors when M and N are about several hundreds to one thousand. Furthermore, the model of parameter noise studied here is similar to that adopted in Ref. [10]; there three noise regimes are distinguished based on the noise correlation time. An important point here is that the main robustness features we found appear in all these three regimes, i.e., do not depend on the noise correlation time. The numerical results shown later correspond to the regime of short noise correlation time as defined in Ref. [10].

Fidelity of single-qubit gates. The Schrödinger equation with the Hamiltonian (1) can be analytically solved, and single-qubit gates U_1 can be achieved, where $\chi = \arctan[\omega_0/(\omega_1-\omega)]$ is the angle between the initial state and the symmetric axis of the rotating field. The corresponding phases for one cycle are given by $\gamma_d = -\pi[\omega_0^2+\omega_1(\omega_1-\omega)]/\omega\Omega$, $\gamma_g = -\pi[1-(\omega_1-\omega)/\Omega]$, and $\gamma = -\pi(1+\Omega/\omega)$ with $\Omega = \sqrt{\omega_0^2+(\omega_1-\omega)^2}$. We can choose any two processes with different values $\{\omega^j,\omega_0^j,\omega_1^j\}$ $(j=1,2)$ satisfying the constrain $\sin\gamma_1\sin\gamma_2\sin(\chi_2-\chi_1)\neq 0$ to enact two noncommuting single-qubit gates [8].

What is remarkable here is that QG U_1 implemented in this way can be varied continuously from a standard dynamic gate to a pure geometric gate, by changing the external parameters $\{\omega,\omega_0,\omega_1\}$. Hence, this scheme looks like an ideal model to compare the difference between geometric QGs and standard dynamic gates. It is straightforward to verify from the expression of γ_d that the dynamic phase (DP) is zero under the condition $\omega = (\omega_0^2+\omega_1^2)/\omega_1$. Thus we can obtain purely geometric gates by choosing these specific parameters, such that $\gamma_d = 0$ in the whole process. It has been shown that χ in U_1 can be controlled independently by the symmetric axis of the rotating field, and a specific QG can be realized by a fixed phase γ [8]. For example, the Hadamard gate is obtained by $\gamma = (n_1+1/2)\pi$ and $\chi = (n_2+1/4)\pi$ (with $n_{1,2}$ integers). Therefore, we assume the total phase is fixed, for concreteness, we choose $\gamma = -\beta\pi$ with β a constant. It is straightforward to check that $\omega = [\omega_1 \pm \sqrt{\omega_1^2-\eta(\omega_0^2+\omega_1^2)}]/\eta$ with $\eta = 2\beta-\beta^2$ guarantee $\gamma = -\beta\pi$. The obvious requirement of ω reality implies $\eta\omega_0^2 \leqslant (1-\eta)\omega_1^2$. On the other hand, the DP is zero under the condition

$$\omega_1 = \omega_0\sqrt{\eta/(1-\eta)}. \qquad (3)$$

The fidelity $F(\omega_0,\Delta)$ and DP of this gate for typical parameters are shown in Fig. 1. Here Δ is defined by $\omega_1 = \sqrt{\eta/(1-\eta)}\omega_0 + \Delta$. $\beta = 3/2$ is chosen just as an example; we have checked that the main results described here are qualitatively similar for different values of the parameter β.

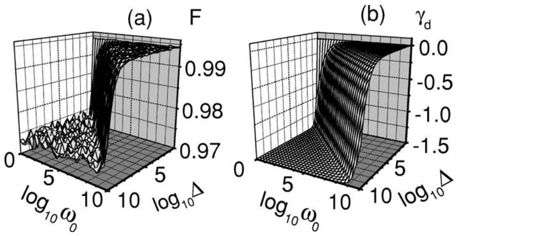

FIG. 1. The fidelity and phase in single-qubit gates: (a) fidelity, (b) dynamic phase.

We plot $F(\omega_0,\Delta)$ instead of $F(\omega_0,\omega_1)$ to guarantee that $\omega[=2(2\omega_1-\sqrt{\omega_1^2-3\omega_0^2})/3]$ is a real number in the whole region. We can see several remarkable features from Fig. 1, where $\delta_0=\delta_1=0.1$: (i) The maximum of fidelity is along the line described by $\Delta=0$, where the DP is zero. (ii) The changes of the absolute value of DPs with Δ are just as the same as the changes of the average fidelity of gates. Therefore, it clearly shows the close relation between the fidelity of QGs and the component of the dynamic (geometric) phase. We also checked the fidelity for different δ_0 and δ_1. The fidelity and quantum phases as a function of Δ for $\omega_0=10^5$ are shown in Fig. 2. We observe that the two main features discussed above appear, for the case $\delta_0=0.1$, when δ_1 is greater than 0.04. However, when δ_1 is less than 0.04, it is worth pointing out that the fidelity in the points with $\Delta=0$ is a local maximum, since there is a dip clearly shown nearby $\Delta\sim\omega_0$; the largest fidelity appears when the DP is dominant. We also numerically computed the fidelity for fixed δ_1 but varied δ_0 (not shown), the main features for different δ_0 are totally similar to those in Fig. 1. The fact that the fidelity is larger when $\Delta(\omega_1)$ is large but with a small fluctuation of ω_1 can be qualitatively explained from the DP γ_d as well as very small fluctuations of the total magnetic field. The deviation of γ_d from the noiseless case is dominated by the fluctuations of ω_1 when Δ is much larger than ω_0. Therefore the infidelity should be small if the fluctuations of ω_1 are very small.

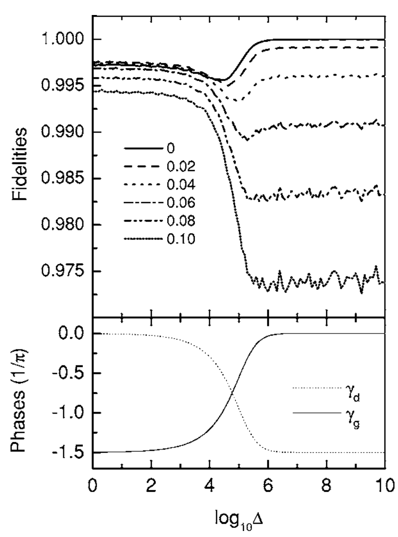

FIG. 2. The fidelities and phases in single qubit gate for $\delta_0=0.1$. The values of δ_1 are indicated: (a) fidelities, (b) dynamic and geometric phases.

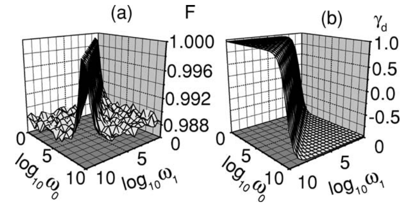

FIG. 3. The fidelity and phase in two-qubit gates for $\delta_0=\delta_1=0.1$, $\delta=0$, and $\alpha=\sqrt{3}$: (a) fidelity, (b) dynamic phase.

Fidelity of two-qubit gates. We now numerically compute the fidelity of a two-qubit gate. We assume that the qubit-qubit interaction is given by $H_I=J\sigma_z^{(1)}\sigma_z^{(2)}/2$. This kind of coupling between qubits can be naturally realized, e.g., in quantum computer models with NMR and superconducting charge qubits coupled through capacitors. When the target qubit is manipulated by a rotating field described by Eq. (1) and the control qubit is off resonance, it is shown that a two-qubit gate $U^{(2)}$ with $\chi^\delta=\arctan[\omega_0/(\omega_1^\delta-\omega)]$ and $\gamma^\delta=-\pi(1+\Omega^\delta/\omega)$ can be implemented. Here $\omega_1^\delta=\omega_1+(2\delta-1)J$ and $\Omega^\delta=\sqrt{\omega_0^2+(\omega_1^\delta-\omega)^2}$, ω, ω_0, and ω_1 are parameters for the target qubit. The corresponding phases for one cycle are given by $\gamma_d^\delta=-\pi[\omega_0^2+\omega_1^\delta(\omega_1^\delta-\omega)]/\omega\Omega^\delta$, and $\gamma_g^\delta=-\pi[1-(\omega_1^\delta-\omega)/\Omega^\delta]$. Besides, it is easy to check from $\gamma_d^\delta=0$ that the geometric two-qubit gates are realized whenever $\omega=2\omega_1$, and $\omega_1^2=\omega_0^2+J^2$ [8].

There is a lot of freedom in choosing parameters to implement a geometric QG in the present scheme. One possible choice is given by $\omega=\omega_1+\sqrt{1+\alpha^2}\omega_0$ and $J=\alpha\omega_0$, thus the speed of the purely geometric gate is of the same order of that of the dynamic gate. To see the relation between the fidelity and the quantum phase, we plot the fidelity and DP of gate U_2 just when $\delta=0$ as a function of ω_0 and ω_1 in Fig. 3. In this case, the DPs change sharply nearby the line described by $\log_{10}\omega_1=\log_{10}(\sqrt{1+\alpha^2}\omega_0)$, where DPs are zero, since it is straightforward to find that under the condition

$$\omega_1=\sqrt{1+\alpha^2}\omega_0, \tag{4}$$

γ_d^δ is zero. We can see from Fig. 3 that the maximum of fidelity is along the line where the DP is zero. Moreover, compared with the single-qubit case shown in Fig. 1, the fidelity of the gate shown here decreases quickly, since the DP changes sharply when the parameters do not satisfy Eq. (4). Therefore, it is clearly shown the close relation between the change of fidelity and the change of dynamic component of the phase.

To show in a more clear fashion that the maximum of fidelity is along the line described by Eq. (4) and that this feature is independent on α, we computed the fidelity of U_2 when the state of the control qubit is unfixed. The fidelity as a function of ω_0 for $\omega_1=60$, $\delta_0=\delta_1=0.05$, and $\alpha=\sqrt{3},\sqrt{8},\sqrt{15},\sqrt{35},\sqrt{143}$ are plotted in Fig. 4. It is easy to derive from Eq. (4) that the DP is zero at $\omega_0=30$, 20, 15, 10, 5, and these points are denoted by arrows in Fig. 4. We observe that the maxima of fidelity are indeed at the points described by Eq. (4), where the DPs are zero; this property is independent on α.

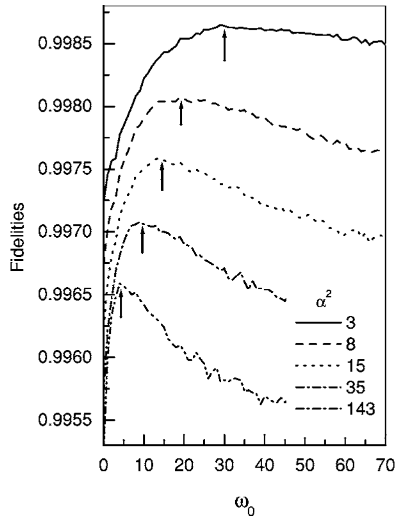

FIG. 4. The fidelities of two-qubit gates. The curves for different α are vertically shifted for clarity. Points with zero dynamic phases shown in Eq. (4) are denoted by arrows.

Comparison with previous results. We would like to compare the results here with the previous results in literature. It has been shown that the effects of fluctuations of the control parameters [12] or decoherence described by Lindblad form [11] on nonadiabatic gates are more severe than for the standard dynamic gates. We note that in Refs. [11,12], the geometric gate is implemented by three rotations, but only one operation is used to realize a standard dynamic gate. Thus a direct comparison is somewhat not appropriate, and one cannot rule out other possibilities. In the present model, however, the operations for both dynamic gate and geometric gate are totally the same, except that the controllable parameters vary continuously. In this sense this model looks definitely more suitable to assess the difference between geometric gates and dynamic gates as far as noise resilience is concerned. We have also computed the fidelity of the gates analyzed in the above in the presence of decoherence described by a Lindblad master equation (just as in Ref. [11]). However, it seems that this noise model is not suitable to distinguish the difference of fidelity between dynamic and geometric gates since, consistently with Ref. [11], we found that the gate fidelity is determined only by the gate operation time, i.e., the dynamical or geometrical nature of the gate is irrelevant.

Finally, we would like to point out that the QC scheme studied in this paper is based on nonadiabatic operations. Note that ω is of the same order of the magnitude as ω_0 or ω_1 in both one- and two-qubit gate operations. This implies that the speed of geometric QG here investigated is comparable with that of the dynamic QG and hence the speed constraint required by adiabatic geometric gates is removed in the present scheme.

This work was supported by the European Union project TOPQIP (Contract No. IST-2001-39215). S.L.Z. was supported by Program for NCET, the NSFC under Grant No. 10204008 and the NSF of Guangdong under Grant No. 021088.

[1] See, e.g., D. P. DiVincenzo and C. Bennett, Nature (London) **404**, 247 (2000).
[2] P. W. Shor, Phys. Rev. A **52**, R2493 (1995); A. M. Steane, Phys. Rev. Lett. **77**, 793 (1996).
[3] L. M. Duan and G. C. Guo, Phys. Rev. Lett. **79**, 1953 (1997); P. Zanardi and M. Rasetti, *ibid.* **79**, 3306 (1997).
[4] L. Viola and S. Lloyd, Phys. Rev. A **58**, 2733 (1998); P. Zanardi, Phys. Lett. A **258**, 77 (1999).
[5] M. V. Berry, Proc. R. Soc. London, Ser. A **392**, 45 (1984); Y. Aharonov and J. Anandan, Phys. Rev. Lett. **58**, 1593 (1987); S. L. Zhu *et al.*, Phys. Rev. B **61**, 1142 (2000).
[6] P. Zanardi and M. Rasetti, Phys. Lett. A **264**, 94 (1999).
[7] J. A. Jones *et al.*, Nature (London) **403**, 869 (2000); L. M. Duan *et al.*, Science **292**, 1695 (2001); Wang Xiang Bin and M. Keiji, Phys. Rev. Lett. **87**, 097901 (2001).
[8] S. L. Zhu and Z. D. Wang, Phys. Rev. Lett. **89**, 097902 (2002); Phys. Rev. A **67**, 022319 (2003).
[9] D. Leibfried *et al.*, Nature (London) **422**, 412 (2003); S. L. Zhu and Z. D. Wang, Phys. Rev. Lett. **91**, 187902 (2003).
[10] P. Solinas *et al.*, Phys. Rev. A **70**, 042316 (2004).
[11] A. Nazir *et al.*, Phys. Rev. A **65**, 042303 (2002).
[12] A. Blais and A.-M. S. Tremblay, Phys. Rev. A **67**, 012308 (2003).
[13] A. Carollo *et al.*, Phys. Rev. Lett. **92**, 020402 (2004); **90**, 160402 (2003).
[14] G. DeChiara and G. M. Palma, Phys. Rev. Lett. **91**, 090404 (2003).
[15] Y. Makhlin *et al.*, Rev. Mod. Phys. **73**, 357 (2001).
[16] L. M. K. Vandersypen and I. L. Chuang, Rev. Mod. Phys. **76**, 1037 (2004).
[17] J. J. Garcia-Ripoll and J. I. Cirac, Phys. Rev. Lett. **90**, 127902 (2003).